

Supplementary Information

Materials and Methods

Materials. The Superdex S200 Increase 10/300 GL column was from GE life sciences (Marlborough, MA). Primary antibodies Total-ERK1/2 (9102S), pERK1/2 (9101S), Src (2109S), pSrc-T416 (6943S), anti-Flag (2368) were from Cell Signaling Technology (Danvers, MA), F431 antibody used to detect Arrestin protein (1), pan-Gi (SC-26761) was from Santa Cruz Biotech., Gs (n192/12) was from EMP Millipore Burlington, MA), HA-tag antibody was from (16B12) Covance (Dedham, MA), GAPDH (AB2302) was from Millipore-sigma (Burlington, MA). HRP-conjugated secondary antibodies (anti-rabbit: 5520-0337, anti-mouse: 55220-0341) were from Seracare (Milford, MA) and anti-goat (sc-2354) was from Santa Cruz Biotech (Dallas, TX). Cell culture media and fetal bovine serum were from Gibco (Waltham, MA). Dopamine hydrochloride was from Abcam (ab120565, Cambridge, MA). Enhanced chemiluminescence substrate (34580) was from ThermoFisher (Waltham, MA). Lipofectamine 2000TM was from Invitrogen (Waltham, MA).

Arrestin-3-(1-393) expression and purification. Arrestin-3 (1-393) was expressed and purified as described (1-5) followed by an additional purification step on a Superdex S200 Increase 10/300 GL column (GE Life Sciences, Pittsburgh, PA) equilibrated in 20 mM MOPS, pH 7.5, 150 mM NaCl, and 2 mM TCEP. Protein purity was assessed by SDS-PAGE with Coomassie staining. Arrestin-3 (1-393) concentrations were determined spectroscopically using corresponding molecular weight (44 kDa) and molar extinction coefficient ($16.5 \times 10^3 \text{ m}^{-1} \text{ cm}^{-1}$) (Synergy Neo2 HTS Multi-Mode Microplate Reader, BioTek).

Expression constructs. For the BRET assays, pcDNA3 encoding Renilla luciferase variant 8 (RLuc8) fused to the D1 receptor C-terminus (6) served as the template for introducing mutations. For a acceptor partner of the BRET, Venus-arrestin fusion construct was used (6). For the ERK1/2 and Src activation assays, pcDNA3 encoding D1R-HA tag was used for introducing mutations. All mutations were confirmed by DNA sequencing (GenHunter DNA Sequencing Service, Nashville, TN).

Peptide Array analysis and Far-western blot. Peptide array synthesis was performed using the ResPep SL peptide synthesizer (Intavis AG, Koeln, Germany) according to standard SPOT synthesis protocols (7, 8). D1R-derived peptides containing 15 amino acids were directly coupled to membranes via the C-terminus during synthesis. Dried membranes with peptides were soaked in 100% ethanol for 5 min then rehydrated in water (twice 5 min). The membranes were blocked for 1 h in Tris-buffered saline (TBS) with 5% milk and 0.05% Tween 20 (Sigma-Aldrich, St. Louis, MO) and washed 3 times (5 min each) in TBS with 0.05% Tween 20 (TBS-T). The membranes were incubated overnight at 4°C with arrestin-3 (1-393) at a final concentration of 0.5 μM in 20 mM MOPS, pH 7.5 buffer containing 150 mM NaCl and 2 mM TCEP. The next morning, membranes were washed 3 times (5 min each) in TBS-T buffer and incubated with primary antibody against arrestin (F431, (9) at 1:5,000 dilution in TBS-T for 1 h). Spots were detected using HRP-conjugated secondary antibodies as described by the manufacturer. For densitometric analysis, the signal in individual dots was quantified as a percentage of total density detected on the membrane (Quantity One and Image Lab, Bio Rad (Hercules, CA), Image J (10)). This allowed for comparison of intensities across all peptide experiments. Statistical analysis was performed using one-way ANOVA followed by Dunnett's post-hoc test using GraphPad Prism 8.0.

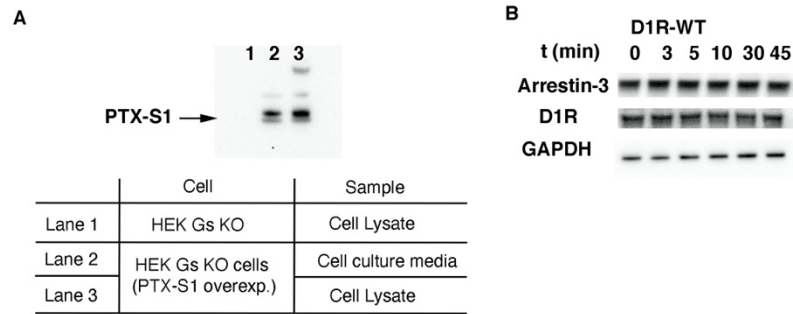
Cell Culture. Arrestin 2/3, Gs and Gi KO HEK293 cells were a gift from Dr. Asuka Inoue (Tohoku University). WT and KO HEK293 cells were maintained in Dulbecco's modified Eagle's media (DMEM) (Invitrogen) supplemented with penicillin (100 IU/ml), streptomycin (100 $\mu\text{g}/\text{ml}$), and 10% (v/v) fetal bovine serum, at 37 °C and 5% CO₂. HEK-293 cells were transfected using a 1:2 DNA:Lipofectamine 2000 (Invitrogen) ratio according to the manufacturer's instructions.

BRET assay. BRET was performed as described previously (6, 11). In brief, the donor was Renilla luciferase variant 8 (RLuc8) C-terminally fused to wild-type or mutant D1R in pcDNA3.1 (6). The acceptor was arrestin-3 with N-terminal Venus in pcDNA3.1(6). HEK-293 cells (80-90% confluent) were co-transfected with Venus-arrestin (0-1 μg), wild-type or mutant RLuc8-D1R (50 ng), and empty pcDNA3.1 (to equalize DNA). The agonist (10 μM dopamine) was added prior to the addition of 5 μM coelenterazine-*h* (12). The net BRET ratio was calculated as the long wavelength emission (530 nm) divided by the short wavelength emission (480 nm) and expressed as the relative change compared with unstimulated cells. The Venus-arrestin-3 fluorescence, which is directly proportional to the

expression level, was normalized by the basal luminescence from the respective D1R-RLuc8 construct (F/L ratio) to account for variations in cell number and expression. For the D1R and G α s interaction, RLuc8-D1R was used as donor and G α s-YFP was used as an acceptor. G α s-YFP was a gift from Dr. Catherine Berlot (Addgene plasmid #55781) (13). For the G α s and arrestin3 interaction, RLuc8-arrestin3 was used as donor and G α s-YFP was used as an acceptor. Net BRET data were fitted to a one-site binding hyperbola or a simple linear regression (when convergence was not achieved). Curve fits and statistical significance ($p < 0.05$) were determined using a Student's t-test or One-Way Analysis of Variance with Tukey's multiple comparison test where appropriate using GraphPad Prism 8.0.

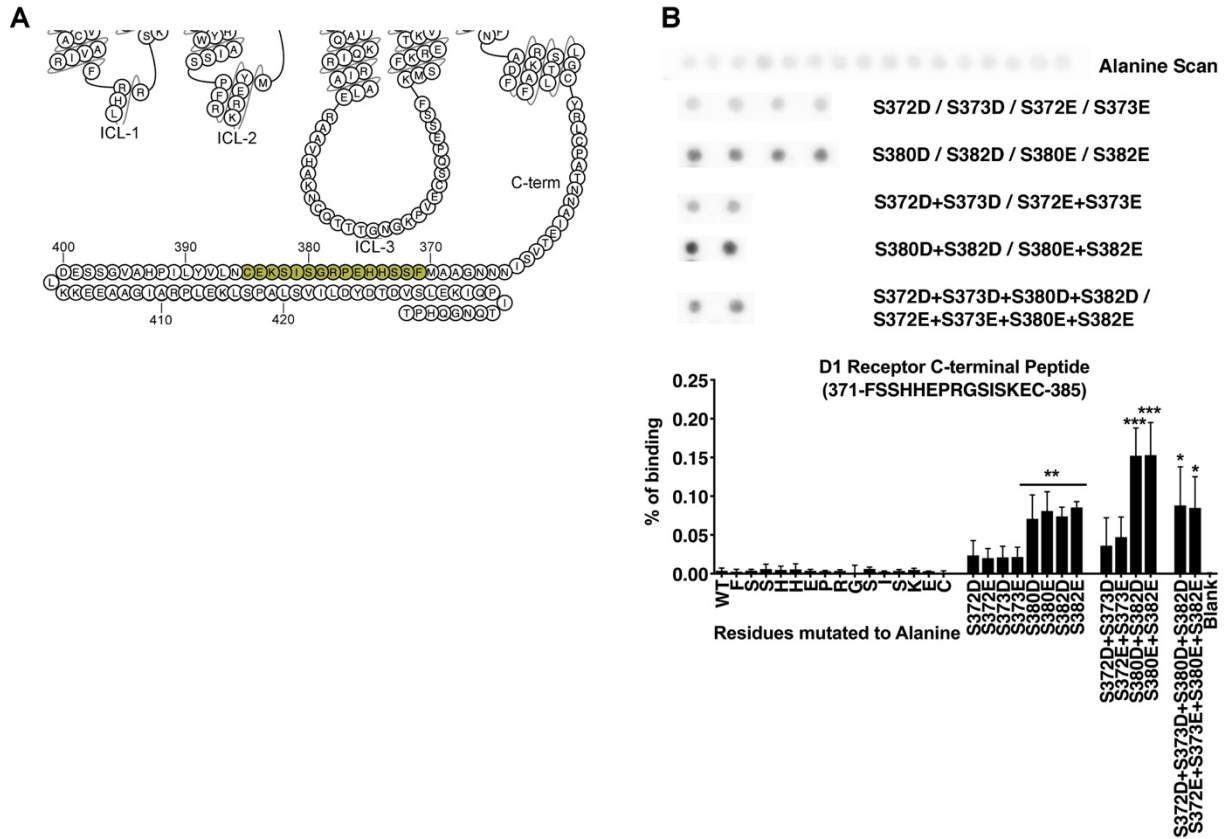
Phosphorylation Assay and Immunoblotting. For the ERK1/2 and Src activation assays, wild-type and mutant D1R with a N-terminal HA tag in pcDNA3.1 was co-transfected with arrestin-3 with a C-terminal HA tag in arrestin-2/3 KO or Gs/G-olf KO HEK293 cell lines. All experiments were conducted 48 h after transfection. For the pertussis toxin expression, Gs/Golf KO HEK293 cells were co-transfected with D1R, arrestin-3, and pcDNA3.1-sf-PTX plasmid 24 h before the experiment (14). In this construct PTX S1 subunit is fused with both a signal peptide and a FLAG tag. After expression, the pertussis toxin is secreted from the cytoplasm and taken back up from the cell media. Cells were serum starved for 16 h and the assay was initiated by adding 10 μ M dopamine. The medium was removed and 400 μ l 2x Laemmli buffer was added. Samples of equal volume from the cell lysates were separated on 4-12% gradient SDS-PAGE, transferred to PVDF membranes and immunoblotted. Signals were quantified by densitometry and expressed as the fold change of unstimulated samples in each experiment. Western Blot images were taken using Biorad ChemiDoc system (BioRad Life Sciences, Hercules,CA). Files were cropped and converted to a JPEG or TIFF file using BioRad Image lab software (BioRad Life Sciences, Hercules,CA). Each figure panel was aligned using Adobe Photoshop CS6 software. Statistical analysis was performed using One-way ANOVA followed by Tukey's post-hoc test for multiple comparisons.

Supplementary Figures

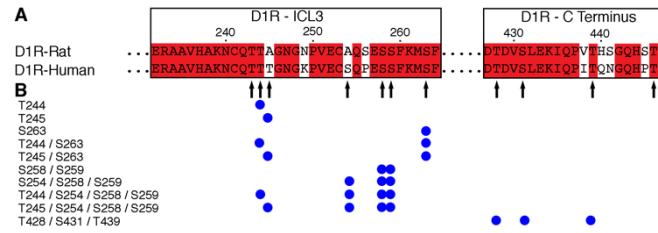


Supplementary Figure 1: Pertussis toxin, Arrestin-3, D1R and GAPDH expression in Gs/Golf KO HEK cells.

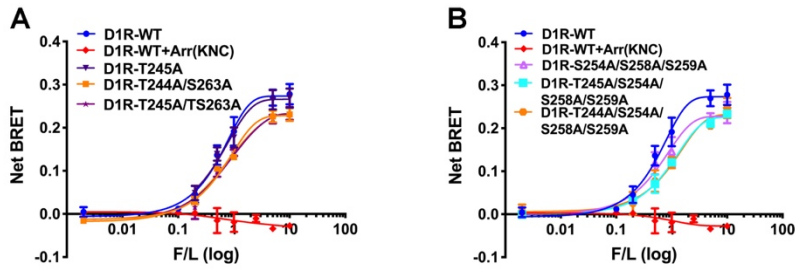
(A) Gs/Golf KO HEK-293 cells co-expressed with D1R, arrestin-3 and PTX. We used pcDNA3.1-SF-hPTX plasmid to express signal peptide and FLAG-tagged PTX S1 subunit in Gs KO HEK-293. After expression, PTX protein is secreted outside of the cell and then taken up from the cell culture media as described (14). PTX expression was detected with an anti-FLAG antibody and Western blotting. (Lane 1) The PTX expression in Gs/Golf KO HEK-293 cell lysate. Lane (2) and (3) are showing Gs/Golf KO HEK-293 cells expressed with PTX. Lane 2 is the sample from cell culture media, Lane 3 is the cell lysate. (B) We used a pan arrestin antibody to detect arrestin-3, an HA antibody to detect D1R, and a GAPDH antibody as an internal control for each sample in our phosphorylation assays. Data repeated with at least three independent experiments and representative images are shown.



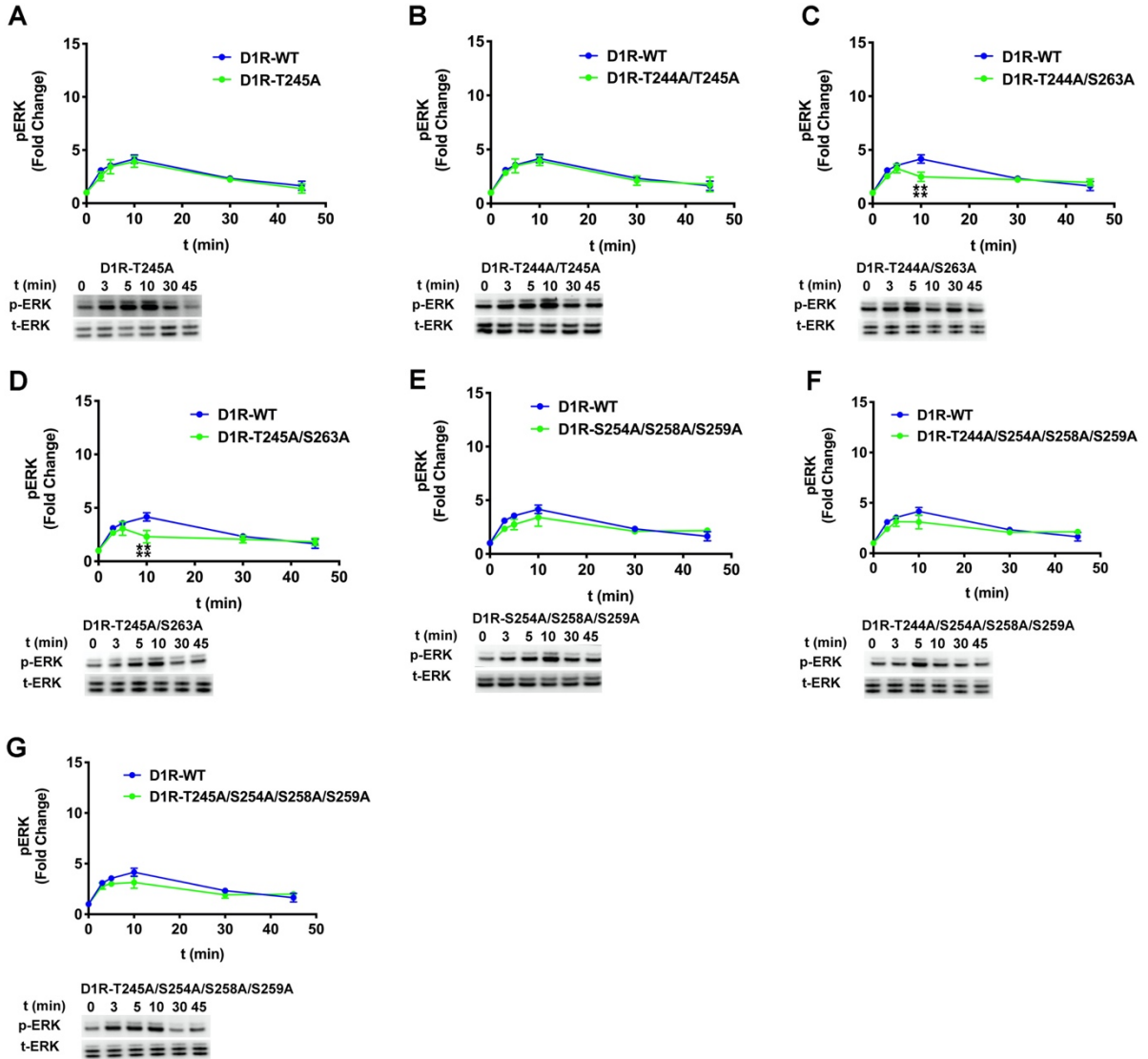
Supplementary Figure 2. Peptide array analysis for the D1R F371-C385 peptide. (A) A snake diagram (15) highlighting the residues that were tested for their role in arrestin-3 binding. (B) Peptide array analysis of the D1R³⁷¹⁻³⁸⁵ peptide. As monitored by Far Western analysis (see Methods), the wild-type peptide exhibited little detectable interaction with arrestin-3; alanine scanning did not significantly impact arrestin-3 binding. Phosphomimetic substitution at positions S380 and S382 increase binding, with an additive effect. However, phosphomimetic substitution of S372 and S373 interfered with this interaction. Data represent at least three independent experiments. Representative peptide array results are shown. Statistical analysis was performed using one-way ANOVA followed by Tukey's post-hoc test. The statistical significance of the difference of the signal from the WT peptide spot is shown, as follows: *, $p < 0.05$; **, $p < 0.01$; ***, $p < 0.001$.



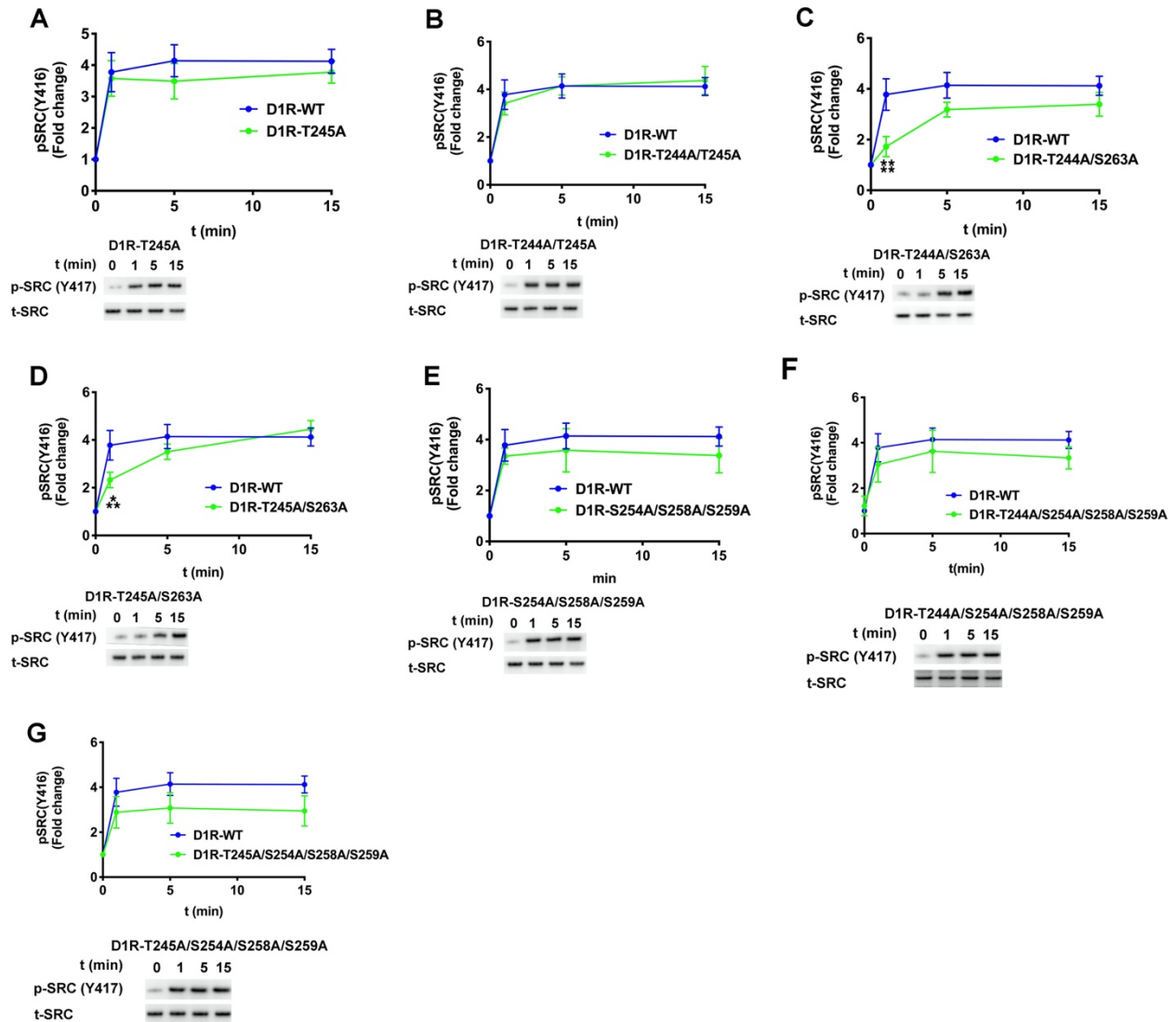
Supplementary Figure 3: Mutagenesis of the D1R intracellular loop 3 and C-terminus. (A) Sequence alignment of the rat and human D1R in the ICL3 and C-terminus. Arrows indicate S/T residues in the ICL3 and the C-terminus of human D1R. (B) Summary of mutations investigated. Blue circles indicate the locations of mutations to alanine or phosphomimetics.



Supplementary Figure 4: In-cell binding of arrestin-3 to WT and mutant D1R. BRET assays were used to measure the binding of wild type and mutant Rluc8-D1Rs to Venus-Arrestin-3 in arrestin2/3 knock-out HEK293 cells (A-B). Mutant D1R receptors were screened in the presence of increasing amounts of Venus-arrestin3 (0-1 μ g) along with 50–100 ng of the plasmid encoding indicated D1R. KNC arrestin (Arr(KNC)) was used as a negative control as it is not capable of binding to receptors (6). The net BRET ratio was calculated as the acceptor emission divided by the donor emission and expressed as the relative change compared with unstimulated cells as describe in the method section. Data represent 3-5 independent experiments.

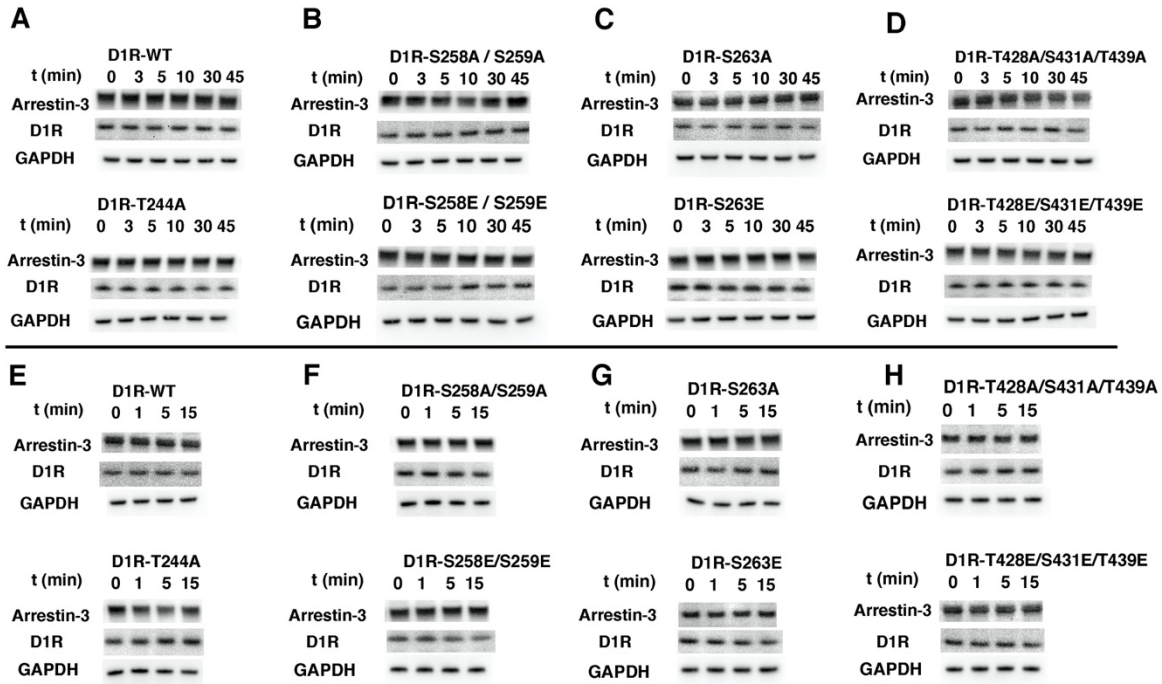


Supplementary Figure 5: D1R phosphorylation pattern affects activation of ERK1/2. Arr2/3 KO HEK-293 cells were overexpressed with D1R and Arrestin-3. The assay was initiated by adding 10 μ M Dopamine at 37 $^{\circ}$ C for the indicated time points. Both phosphorylated ERK (pERK) and total ERK (tERK) were visualized by Western blotting. Cell lysates were separated on 4-12% gradient SDS-PAGE, transferred to PVDF membranes and immunoblotted using the indicated antibody. Signals were quantified by densitometry and expressed as the fold change of unstimulated samples in each experiment. Representative images are shown for each receptor mutant group. Data represents at least three independent experiments. Statistical analysis was determined with one-way ANOVA followed by Tukey's post hoc test with correction for multiple comparisons between WT- and mutant receptor mediated signal in each time points (***) $P < 0.001$.

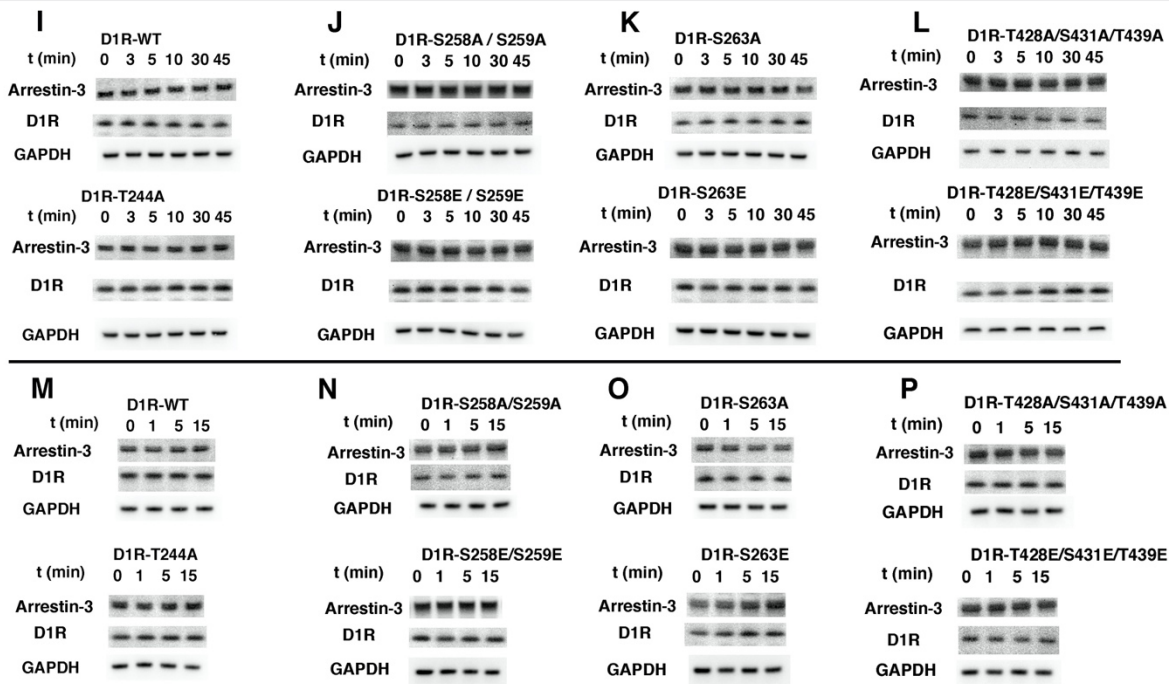


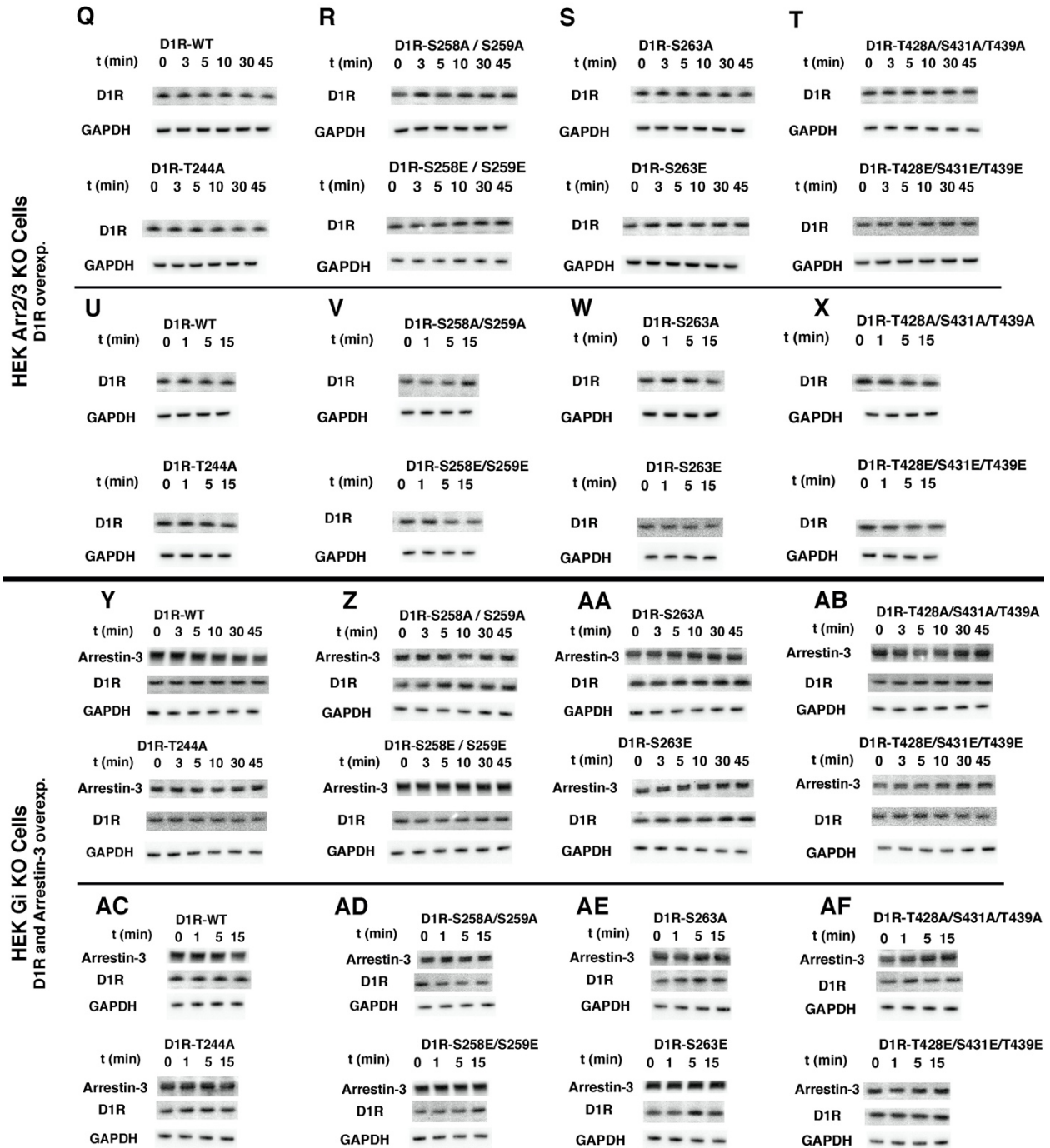
Supplementary Figure 6: The effect of phosphorylation pattern of D1R on the Src activation. Arr2/3 KO HEK-293 cells were overexpressed with D1R and arrestin-3. The assay was initiated by adding 10 μ M Dopamine at 37 $^{\circ}$ C for indicated time points. Both phosphorylated SRC (pSRC) and total SRC (tSRC) were visualized by Western blotting. Cell lysates were separated on 4-12% gradient SDS-PAGE, transferred to PVDF membranes and immunoblotted using the indicated antibody. Signals were quantified by densitometry and expressed as the fold change of unstimulated samples in each experiment. Representative images are showing from each receptor mutant group. Data represents at least three independent experiments. Statistical analysis was determined with one-way ANOVA followed by Tukey's post hoc test with correction for multiple comparisons between WT- and mutant receptor mediated signal in each time points (** $P < 0.001$; *** $P < 0.0001$).

HEK Arr2/3 KO Cells
D1R and Arrestin-3 overexp.

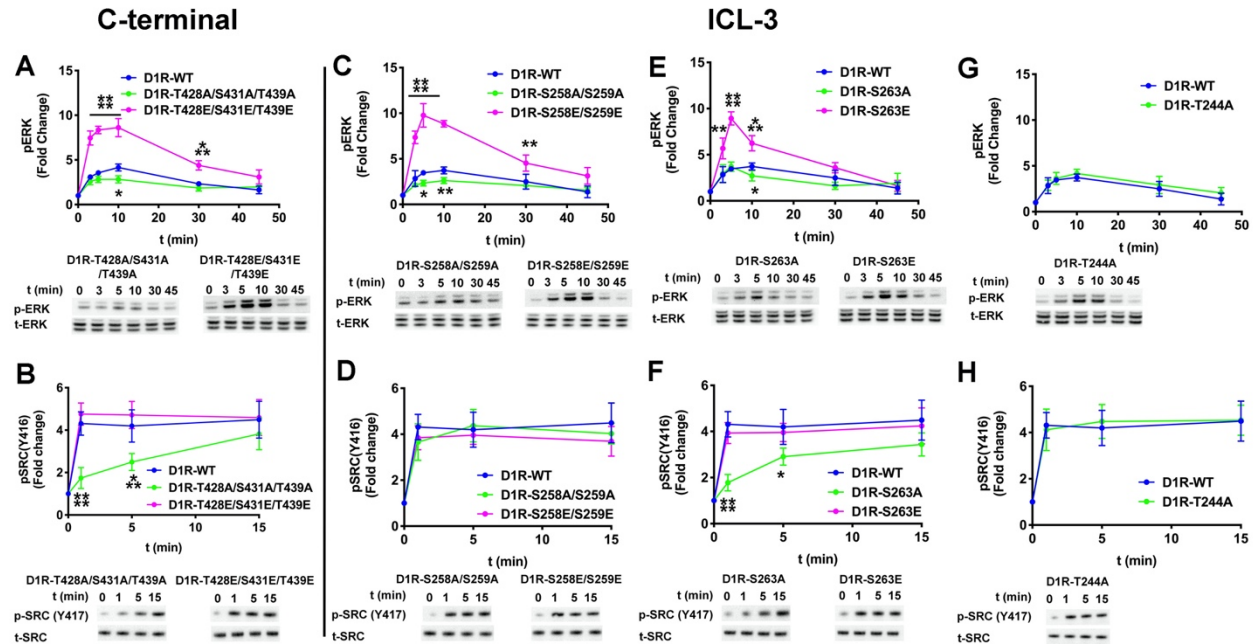


HEK Gs KO Cells
D1R and Arrestin-3 overexp.

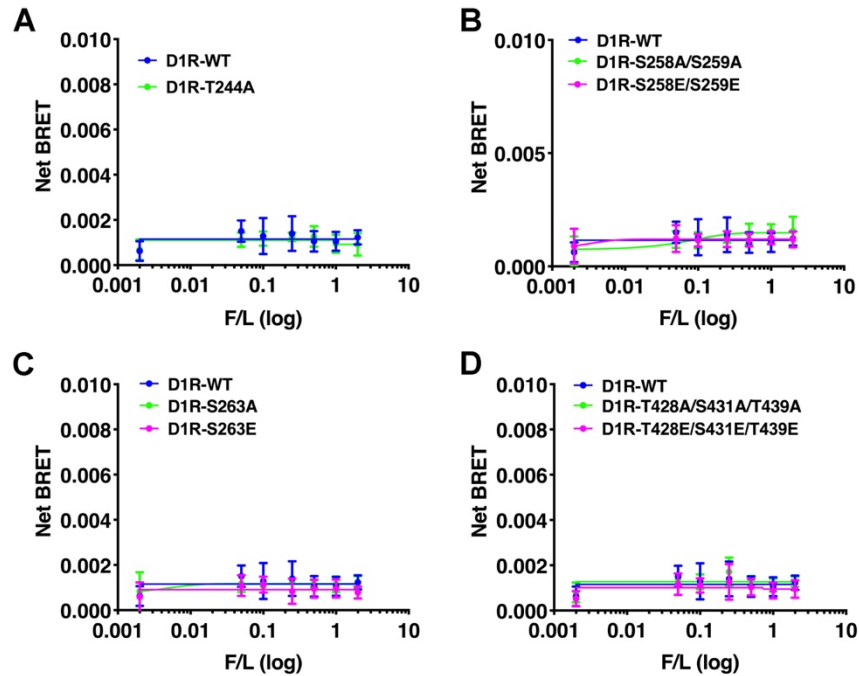




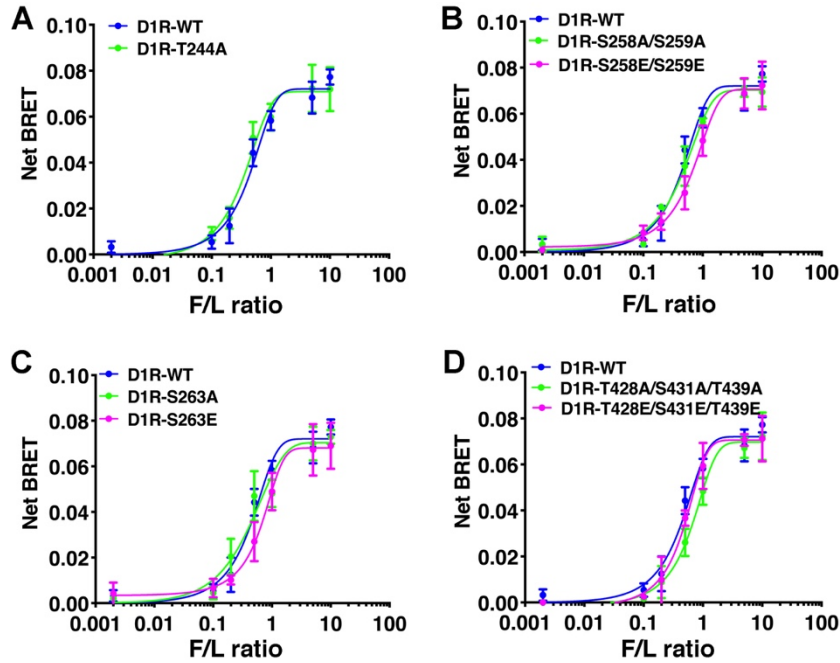
Supplementary Figure 7: Arrestin-3, D1R and GAPDH expression levels in HEK cells. We used an arrestin antibody to detect arrestin-3, HA antibody to detect D1R and GAPDH antibody as an internal control for each sample in our phosphorylation assays. The samples from the Arr2/3 KO HEK-293 cells co-expressed with D1R and Arrestin-3, the Gs KO HEK-293 cells co-expressed with D1R and the Arrestin-3, Arr2/3 KO HEK-293 cells expressed with D1R, Gi KO HEK-293 cells co-expressed with D1R and the Arrestin-3 are showing in the first, second, third and fourth panel, respectively. GAPDH detected with anti-GAPDH antibody by using Western blotting. Data repeated with at least three independent experiments and representative images are showing from each sample.



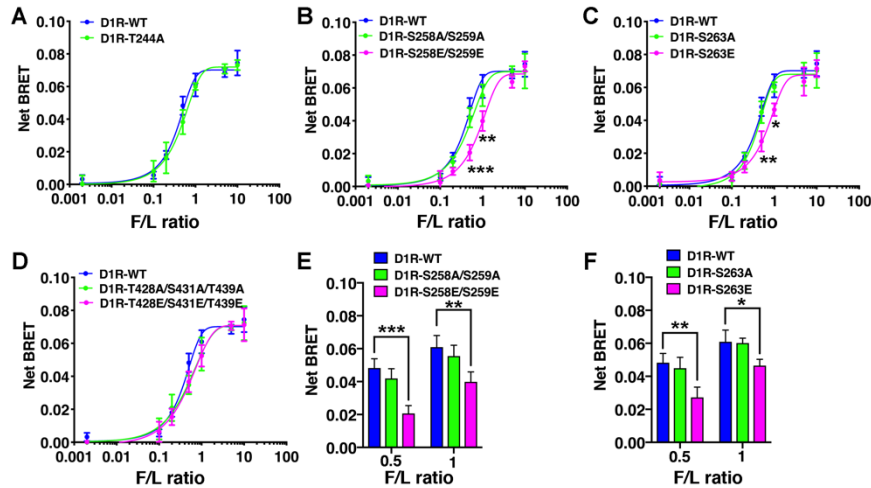
Supplementary Figure 8: The effect of the D1R-ICL3 phosphorylation pattern on ERK1/2 and Src kinase phosphorylation. *Gai/o/t* KO HEK-293 cells were co-transfected with plasmids encoding arrestin-3 and either wild-type or variant D1R. The assay was initiated by adding 10 μ M dopamine at 37 $^{\circ}$ C. Cell lysates were separated on a 4–12% gradient SDS-PAGE, transferred to PVDF membranes and immunoblotted for phosphorylated ERK1/2 (pERK), phosphorylated Src (pSrc), total ERK1/2 (tERK), and total Src (tSRC). Signals were quantified by densitometry and expressed as the fold change relative to unstimulated samples in each experiment. (A) – (D) Time course of ERK 1/2 phosphorylation associated with dopamine stimulation of cells expressing wild-type or variant D1R. (E) – (H) Time course of Src kinase activation associated with dopamine stimulation of cells expressing wild-type or variant D1R. Data represent at least three independent experiments. GAPDH expression was used as an internal control for each sample (SI Appendix Fig. S6). Statistical analysis was performed with one-way ANOVA followed by Tukey’s post hoc test with correction for multiple comparisons between wild-type and mutant D1R mediated signal at each time point. Significance is shown, as follows: *, $p < 0.05$; **, $p < 0.01$; ***, $p < 0.001$; ****, $p < 0.0001$.



Supplementary Figure 9: In-cell proximity between arrestin-3 and G α s suggests against formation of a D1R-Gs-arrestin-3 super complex A BRET assay was used to measure the proximity between Rluc8-Arrestin3 and G α s-YFP in the presence of WT and mutant D1R in the arrestin-2/3 KO HEK293 cells as described in method section. (A) – (D) BRET signal of wild-type and variant D1R receptors stimulated by 10 μ M dopamine in the presence of increasing amounts of G α s-YFP (0-1 μ g) and monitored for 10 min. The net BRET ratio was calculated as the acceptor emission divided by the donor emission and expressed as the relative change compared with unstimulated cells. Statistical analysis was performed using one-way ANOVA followed by Tukey’s post-hoc test and we didn’t find any statistical differences.



Supplementary Figure 10: In-cell binding of $G\alpha_s$ to WT and mutant D1R in the absence of arrestin. A BRET assay was used to measure the binding between WT and mutant Rluc8-D1R to $G\alpha_s$ -YFP in arrestin-2/3 KO HEK293 cells as described in the legend to Fig. 4. (A) – (D) BRET signal of wild-type and variant D1R receptors stimulated by 10 μ M dopamine in the presence of increasing amounts of $G\alpha_s$ -YFP (0-1 μ g) and monitored for 10 min. The net BRET ratio was calculated as the acceptor emission divided by the donor emission and expressed as the relative change compared with unstimulated cells. Statistical analysis was performed using one-way ANOVA followed by Tukey's post-hoc test and we didn't find any statistical differences.



Supplementary Figure 11: In-cell binding of $G\alpha_s$ to WT and mutant D1R in the presence of overexpressed arrestin-3. A BRET assay was used to measure the binding between WT and mutant D1R-Rluc8 to $G\alpha_s$ -YFP. (A) – (D) BRET signal of wild-type and mutant D1R stimulated by 10 μ M dopamine in the presence of increasing amounts of $G\alpha_s$ -YFP (0–1 μ g) monitored for 10 min. The net BRET ratio was calculated as the acceptor emission divided by the donor emission and expressed as the change relative to unstimulated cells. Statistical analysis was performed using one-way ANOVA followed by Tukey’s post-hoc test. (E) The statistical significance of the signal detected at the indicated donor acceptor ratios between the WT-D1R and the D1R-S258E-S259E (**, $p < 0.01$, ***, $p < 0.001$). (F) The statistical significance of the signal detected at the indicated donor acceptor ratios between the WT-D1R and the D1R-S263E (*, $p < 0.05$, **, $p < 0.01$).

References

1. S. A. Vishnivetskiy, X. Zhan, Q. Chen, T. M. Iverson, V. V. Gurevich, Arrestin expression in *E. coli* and purification. *Curr Protoc Pharmacol* **67**, Unit 2.11.11-19 (2014).
2. J. M. Pleinis, C. W. Davis, C. B. Cantrell, D. Y. Qiu, X. Zhan, Purification, auto-activation and kinetic characterization of apoptosis signal-regulating kinase I. *Protein Expression and Purification* **132**, 34-43 (2017).
3. X. Zhan, T. S. Kaoud, K. N. Dalby, V. V. Gurevich, Non-visual arrestins function as simple scaffolds assembling the MKK4–JNK3a2 signaling complex. *Biochemistry* **50**, 10520-10529 (2011).
4. C. Yan, T. Kaoud, S. Lee, K. N. Dalby, P. Ren, Understanding the Specificity of a Docking Interaction between JNK1 and the Scaffolding Protein JIP1. *The Journal of Physical Chemistry B* **115**, 1491-1502 (2011).
5. Q. Chen *et al.*, Structural basis of arrestin-3 activation and signaling. *Nat Commun* **8**, 1427 (2017).
6. L. E. Gimenez *et al.*, Role of receptor-attached phosphates in binding of visual and non-visual arrestins to G protein-coupled receptors. *J Biol Chem* **287**, 9028-9040 (2012).
7. R. Frank, The SPOT-synthesis technique. Synthetic peptide arrays on membrane supports—principles and applications. *J Immunol Methods* **267**, 13-26 (2002).
8. Y. Y. Yim, K. Betke, H. Hamm, Using peptide arrays created by the SPOT method for defining protein-protein interactions. *Methods Mol Biol* **1278**, 307-320 (2015).
9. E. Alvarez-Curto *et al.*, Targeted Elimination of G Proteins and Arrestins Defines Their Specific Contributions to Both Intensity and Duration of G Protein-coupled Receptor Signaling. *J Biol Chem* **291**, 27147-27159 (2016).
10. C. A. Schneider, W. S. Rasband, K. W. Eliceiri, NIH Image to ImageJ: 25 years of image analysis. *Nat Methods* **9**, 671-675 (2012).
11. X. Zhan, L. E. Gimenez, V. V. Gurevich, B. W. Spiller, Crystal structure of arrestin-3 reveals the basis of the difference in receptor binding between two non-visual subtypes. *J Mol Biol* **406**, 467-478 (2011).
12. S. Marullo, M. Bouvier, Resonance energy transfer approaches in molecular pharmacology and beyond. *Trends Pharmacol Sci* **28**, 362-365 (2007).
13. E. A. Yost, S. M. Mervine, J. L. Sabo, T. R. Hynes, C. H. Berlot, Live cell analysis of G protein beta5 complex formation, function, and targeting. *Mol Pharmacol* **72**, 812-825 (2007).
14. S. R. Ikeda, S. W. Jeong, P. J. Kammermeier, V. Ruiz-Velasco, M. M. King, Heterologous expression of a green fluorescent protein-pertussis toxin S1 subunit fusion construct disrupts calcium channel modulation in rat superior cervical ganglion neurons. *Neurosci Lett* **271**, 163-166 (1999).
15. V. Isberg *et al.*, GPCRdb: an information system for G protein-coupled receptors. *Nucleic Acids Res* **45**, 2936 (2017).